Multi-Link Operation in Heterogeneous Wi-Fi 7 Networks: Modeling and Throughput Optimization

Wenhai Lin*†, Xinghua Sun*, Wen Zhan*, and Yuan Jiang*†
*School of Electronics and Communication Engineering, Sun Yat-sen University, Shenzhen 518107, China.
† Guangdong Provincial Key Laboratory of Sea-Air-Space Communication, Shenzhen 518107, China.
Email: linwh33@mail2.sysu.edu.cn, {sunxinghua, zhanw6, jiangyuan3}@mail.sysu.edu.cn

2025 IEEE Wireless Communications and Networking Conference (WCNC) | 979-8-3503-6836-9/25/$31.00 ©2025 IEEE | DOI: 10.1109/WCNC61545.2025.10978223

***Abstract*—Multi-link operation (MLO) is regarded as one of the most disruptive features in the upcoming IEEE 802.11be standard, known as Wi-Fi 7. However, the performance characterization of heterogeneous multi-link IEEE 802.11be networks, which consist of Multi-Link Devices (MLDs) and legacy Single-Link Devices (SLDs), remains largely unknown. The challenge originates from the lack of proper modeling of multi-link channel access schemes. In this paper, a novel model is established to study the throughput optimization of heterogeneous two-link IEEE 802.11be networks. MLDs adopt one representative synchronous multi-link channel access scheme with the primary channel. Based on the proposed model, explicit expressions of throughput of MLDs and legacy SLDs are both characterized and verified by simulation results. The network throughput is further maximized by optimally choosing the transmission probabilities of SLDs and MLDs. The analysis shows that MLO can enable MLDs to achieve higher device throughput than SLDs, yet the maximum network throughput of heterogeneous networks decreases compared to homogeneous networks composed solely of MLDs or legacy SLDs.**

***Index Terms*—IEEE 802.11be, multi-link operation, random access, performance optimization**

I. Introduction

To meet the requirements of the emerging ultra-high throughput and stringent low-latency applications, including augmented reality (AR) and virtual reality (VR), the Task Group BE (TGbe) is working on the next generation IEEE 802.11be standard, also known as Wi-Fi 7 [1], [2]. In IEEE 802.11be, TGbe introduced multiple channels across 2.4 GHz, 5 GHz, and 6 GHz. To enable feasible and efficient utilization of multiple available links, multi-link operation (MLO) is suggested as a key candidate feature of Wi-Fi 7 [3]. With MLO, a Multi-Link Device (MLD) can transmit data on multiple links simultaneously, facilitating the attainment of both tremendous data rates and extremely low latency.

This work was supported in part by the National Key Research and Development Program of China under Grant 2023YFB2904100, in part by Guangdong Basic and Applied Basic Research Foundation under Grant 2024A1515012015, in part by the Fundamental Research Funds for the Central Universities, Sun Yat-sen University, under Grant 24pnpy204, and in part by the Open Fund of State Key Laboratory of Satellite Navigation System and Equipment Technology (No. CEPNT-2021KF-04).

In the current IEEE 802.11be standard, MLDs are expected to independently access and transmit on each link to maximize the gain of multiple links. However, it is challenging for client MLDs to access each link independently. This is because independent access requires MLDs to have simultaneous transmission and reception (STR) capability, e.g., the capability to transmit on one link and receive the signal on another link. STR capability necessitates MLDs to handle power leakage resulting from insufficient frequency separation. Yet typical client MLDs, which tend to be cheap and are equipped with simple filters, are difficult to eliminate power leakage through physical layer (PHY) technology and therefore can only operate multiple links in a constrained manner.

To enable the utilization of multiple links for STR-inability (NSTR) MLDs, one feasible way is to design a synchronous medium access control (MAC) protocol that ensures all transmissions over multiple links start and end synchronously. Numerous synchronous MAC protocols for Wi-Fi 7 have been proposed [4], [5]. In particular, the scheme proposed in [4] inherited the wideband operation of 802.11 and introduced one primary link and several secondary links. According to this scheme, MLDs contend only on a selected primary link. When an MLD obtains a transmission opportunity on the primary link, it can aggregate the primary link with all the idle secondary links and transmit on the aggregated link. The access scheme based on the primary channel has attracted widespread research interest and is also the focus of this paper.

Although the synchronous MAC protocol cannot access each channel independently, extensive simulation and analytical studies have confirmed that the synchronous MAC protocol can substantially enhance throughput and reduce latency in homogeneous networks [6], [7], which consist only of MLDs. In practice, however, the MLDs inevitably coexist with legacy Single-Link Devices (SLDs), and the throughput performance of MLDs is strongly affected by the presence of legacy SLDs [8]. The presence of legacy SLDs reduces the opportunities for plural transmission via several links. Therefore, it is highly desirable to study the performance of heterogeneous networks, consisting of both MLDs and SLDs.

In heterogeneous networks with synchronous MAC protocols for MLDs, the characterization of the network performance becomes intricate due to the correlation between the behaviors of SLDs on different links. For instance, consider two links: the transmission of SLDs on link 1 can block the transmission of MLDs on both links, allowing SLDs on link 2 to gain more transmission opportunities. This phenomenon, which we refer to as *inter-link coupling*, is caused by the fact the synchronous transmission of MLD creates strong correlation among links. Several analytical models [9], [10], [11] have been developed for heterogeneous networks by extending the classic Bianchi model [12]. However, these models marginalized or neglected the effects of inter-link coupling. In particular, the access of SLDs on different links was treated as independent. As a result, the behavior of SLDs on different links was modeled using separate Markov Chains in [12], without considering the correlations between them. Moreover, the adopted Bianchi model was originally designed for single-link networks and *lacked the ability to capture the coupling of SLDs across multiple links*. That calls for clean-slate modeling for heterogeneous networks with inter-link coupling, based on which the network performance, such as network throughput, can be characterized and further optimized.

In this paper, a novel analytical model is proposed for throughput optimization of multi-link heterogeneous IEEE 802.11be networks. Specifically, we consider MLDs adopting the synchronous channel access scheme based on the primary channel [4]. A discrete-time Markov renewal process is established to model the state transition of this multi-link network. Due to the inter-link coupling, the state transitions of each link should be considered collectively rather than individually. Therefore, we design a high-dimensional state characterization for the multi-link network, which includes the state of each link and a variable to describe the initiation timing of the state of each link. Based on the proposed model, we characterize the probability of channels being idle and the throughput of various devices as functions of the number and the transmission probability of each type of device. The network throughput is further optimized by optimally choosing the transmission probabilities of SLDs and MLDs. The analysis reveals that the maximum network throughput is closely determined by the transmission probability of legacy SLDs. Although MLDs can achieve higher device throughput than SLDs, the maximum network throughput of heterogeneous networks is lower than that of homogeneous networks consisting solely of MLDs or legacy SLDs.

The rest of the paper is organized as follows: a novel model for heterogeneous multi-link IEEE 802.11be network is proposed in Section II. Based on this, the throughput characterization and optimization are studied in Section III. Section IV presents simulation results. Finally, concluding remarks are summarized in Section V.

II. System Model

Consider a two-link[1] heterogeneous IEEE 802.11be network with n_{S1}-node legacy SLDs transmitting on link 1, n_{S2}-node legacy SLDs transmitting on link 2, and n_M-node MLDs transmitting on both links.

To support synchronous channel access for each MLD, numerous access methods have been considered by TGbe [4], [5]. In this paper, we consider the representative scheme proposed in [4]. In this scheme, MLDs classify the links into one primary link and several secondary links. MLDs perform the Distributed Coordination Function (DCF) protocol only on the primary channel. Specifically, when each MLD has packet to transmit, it randomly selects a backoff counter from $\{0, 1, \ldots, CW_{i-1}\}$, where $CW_i = CW \cdot 2^{\min(i,K)}$ is the backoff window size, which doubles with each collision encountered by the node until the collision counter i reaches the cutoff phase K. Whenever the primary channel is idle, the backoff counter is decremented by one. When the backoff counter reaches zero, the MLD will aggregate the links that are sensed as idle and transmit over the aggregated channel. Let SLD i denote the legacy SLDs on the i-th link. Each SLD performs the DCF protocol on its respective link for transmission.

Assume the network is time slotted. The time axis is divided into multiple time slots. Each node requires one time slot to sense the channel. Transmissions can be initiated only at the beginning of a time slot, and successful and failed packet transmissions both last for τ time slots. The classic collision model is adopted at the receiver. That is when multiple nodes transmit their packets simultaneously on a link, a collision occurs, and none of them can be successfully decoded.

In this paper, we consider a saturated network[2], where the buffer of each node in the network is always non-empty. Note that in throughput performance analysis of a saturated network, the DCF protocol, where each node's access depends on its initial backoff window W and cutoff phase K, can be equivalent to the node attempting transmission with a certain probability q whenever the channel is sensed as idle. This probability q can be determined as a function of W and K. Specifically, when $K = 0$, we have $q = \frac{2}{W+1}$ [13]. In this paper, we adopt this equivalence. Assume that q_M, q_{S1}, and q_{S2} are the transmission probabilities of MLDs, SLD 1, and SLD 2, respectively.

A. Network Throughput

Due to uncoordinated transmissions of nodes, the number of successfully decoded packets varies from time to time. For

[1]Note that, for ease of exposition, we focus on scenarios involving only two links. This scenario is crucial, as near-future smartphones are unlikely to feature more than two Wi-Fi radios [9]. Furthermore, the modeling approach is also applicable to more links.

[2]This paper focuses on throughput optimization, thus placing greater emphasis on the saturated condition, where network throughput is pushed to its limits.

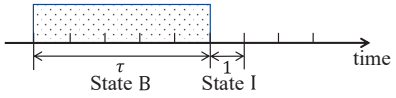

Fig. 1. Channel states in the multi-link network.

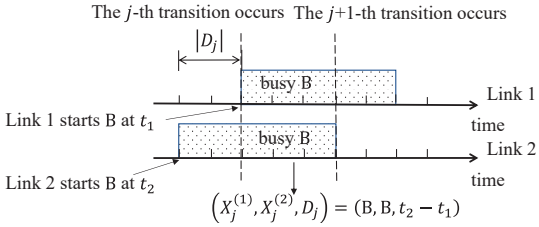

Fig. 2. Illustration of the definition and calculation of D_j.

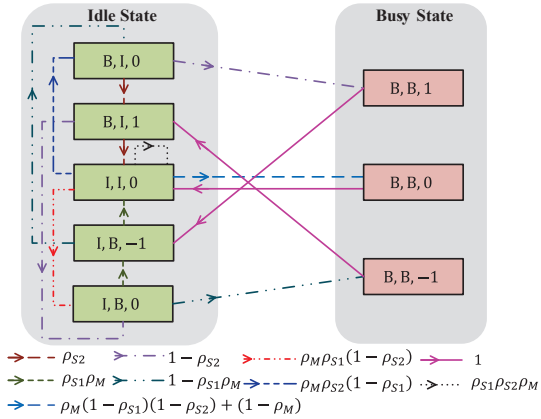

Fig. 3. Embedded Markov chain $\{\boldsymbol{X}_j\}$ given $\tau = 2$.

each type of device in random-access networks, the average number of successfully decoded packets per time slot is an important performance metric, which is referred to as the device throughput and reflects the access efficiency.

The network throughput $\hat{\lambda}_{out}^{total}$ is the sum of all the device throughput, which can be written as

$$\hat{\lambda}_{out}^{total} = \hat{\lambda}_{out}^{S1} + \hat{\lambda}_{out}^{S2} + \hat{\lambda}_{out}^{M}, \tag{1}$$

where $\hat{\lambda}_{out}^{S1}$, $\hat{\lambda}_{out}^{S2}$, and $\hat{\lambda}_{out}^{M}$ are the throughput of SLD 1, SLD 2, and MLDs, respectively. Specifically, the throughput of MLDs is equal to the sum of the fraction of the time during which link 1 is in the MLD successful packet transmission state and that during which link 2 is in the MLD successful packet transmission state. When two channels are idle, the MLD would transmit two distinct packets on both channels. If both packets are successfully decoded, then the MLD obtains a doubled throughput, indicating the throughput of one MLD could be greater than one. The key to throughput analysis lies in the characterization of the probabilities of the channel being in different states. A multi-link model is established to characterize the channel state transition of multi-link networks, which will be described in detail in the following subsection.

B. Multi-Link Modeling

The channel state transition of the two-link network can be modeled as a discrete-time Markov renewal process, i.e., $(\boldsymbol{\mathcal{X}}, \boldsymbol{V}) = \{(\boldsymbol{X}_j, V_j), j = 0, 1, \ldots\}$, where V_j denotes the epoch at which the j-th transition occurs, and $\boldsymbol{X}_j$ represents the state of the multi-link network after the j-th transition. The state of multi-link network $\boldsymbol{X}$ needs to describe the state and the initiation timing of the state of each link. Therefore, $\boldsymbol{X}$ is composed as follows:

$$\boldsymbol{X}_j = \left(X_j^{(1)}, X_j^{(2)}, D_j\right), \tag{2}$$

where $X_j^{(i)}$ denotes the states of the i-th channel after the j-th transition. Fig. 1 illustrates two states of the link: busy (State B)[3] and idle (State I), which lasts for τ time slots and 1 time slot, respectively. The third term in (2), D_j, is a variable that characterizes the initiation timing of the state of each link. Specifically, D_j is defined as the time difference in the initiation timing of the states between the two links at the j-th transition (in the unit of time slot). Fig. 2 illustrates the definition and calculation of D_j.

The dimension of the embedded Markov chain $\boldsymbol{\mathcal{X}} = \{\boldsymbol{X}_j\}$ is closely correlated with τ. In the following, we will present an example of $\tau = 2$ to demonstrate the state transition process of $\boldsymbol{\mathcal{X}} = \{\boldsymbol{X}_j\}$. As Fig. 3 illustrates, ρ_{S1}, ρ_{S2} and ρ_M represent the probabilities that SLD 1, SLD 2 and MLDs, do not transmit upon sensing the corresponding channels idle, respectively, which are

$$\rho_{S1} = (1 - q_{S1})^{n_{S1}}, \rho_{S2} = (1 - q_{S2})^{n_{S2}}, \rho_M = (1 - q_M)^{n_M}. \tag{3}$$

Let $\mathbb{S}$ denote the state space of $\boldsymbol{\mathcal{X}}$. The probability of the coexisting network transitioning from the State $\boldsymbol{\nu} \in \mathbb{S}$ to the State $\boldsymbol{\mu} \in \mathbb{S}$ in one step is $p_{\boldsymbol{\nu},\boldsymbol{\mu}}$. The transition probability from the State $\boldsymbol{\nu}$ to the State $\boldsymbol{\mu}$ is solely determined by $\boldsymbol{\nu}$ and $\boldsymbol{\mu}$, and it can be obtained using conditional probability. For instance, in Fig. 3, the probability of the transition from $(\mathrm{I}, \mathrm{B}, 0)$ to $(\mathrm{I}, \mathrm{B}, -1)$ is [4]

$$p_{(\mathrm{I},\mathrm{B},0),(\mathrm{I},\mathrm{B},-1)} = \Pr\{(\mathrm{I}, \mathrm{B}, -1) \,|(\mathrm{I}, \mathrm{B}, 0)\} = \rho_{S1}\rho_M, \tag{4}$$

where the State $(\mathrm{I}, \mathrm{B}, 0)$ indicates that only link 1 is idle, where only SLD 1 and MLDs can transmit in the next time slot. Then the probability that no nodes request to transmit given that link 1 is idle and link 2 is busy at the previous time slot is $\rho_{S1}\rho_M$. Therefore, the transition probability is $\rho_{S1}\rho_M$.

The steady-state probability distribution for the embedded Markov chain $\boldsymbol{\mathcal{X}} = \{\boldsymbol{X}_j\}$ can be derived by

$$\begin{cases} \pi_{\boldsymbol{\mu}} = \sum_{\boldsymbol{\nu} \in \mathbb{S}} p_{\boldsymbol{\nu},\boldsymbol{\mu}} \pi_{\boldsymbol{\nu}}, \\ 1 = \sum_{\boldsymbol{\mu} \in \mathbb{S}} \pi_{\boldsymbol{\mu}}, \end{cases} \tag{5}$$

[3]Busy state contains both successful and failed packet transmission state.

[4]We adopt the short notation: $\Pr\{\boldsymbol{\nu} \,|\boldsymbol{\mu}\} = \Pr\{\boldsymbol{X}_{j+1} = \boldsymbol{\nu} \,|\boldsymbol{X}_j = \boldsymbol{\mu}\}$, where $\boldsymbol{\nu}, \boldsymbol{\mu} \in \mathbb{S}$.

where $\pi_{\boldsymbol{\mu}}$ is the steady-state probability of $\boldsymbol{\mu}$.

Note that the limiting state probabilities of the Markov renewal process $(\boldsymbol{\mathcal{X}}, \boldsymbol{V})$ are given by

$$\tilde{\pi}_{\boldsymbol{\mu}} = \frac{\pi_{\boldsymbol{\mu}} \cdot \tau_{\boldsymbol{\mu}}}{\sum_{\boldsymbol{\nu} \in \mathbb{S}} \pi_{\boldsymbol{\nu}} \cdot \tau_{\boldsymbol{\nu}}}, \tag{6}$$

$\boldsymbol{\mu} \in \mathbb{S}$, where $\tau_{\boldsymbol{\mu}}$ denotes the holding time of the State $\boldsymbol{\mu}$ (in the unit of time slot). For State $(\mathrm{I}, \mathrm{I}, 0)$, $(\mathrm{I}, \mathrm{B}, D)$ and $(\mathrm{B}, \mathrm{I}, D)$, we have

$$\tau_{(\mathrm{I},\mathrm{I},0)} = \tau_{(\mathrm{B},\mathrm{I},D)} = \tau_{(\mathrm{I},\mathrm{B},D)} = 1. \tag{7}$$

Regarding State $(\mathrm{B}, \mathrm{B}, D)$, the holding time is given by

$$\tau_{(\mathrm{B},\mathrm{B},D)} = \tau - |D|, \tag{8}$$

where $|\cdot|$ is the absolute value function.

The device throughput can be derived from the limiting state probabilities of the States where at least one of the links is idle[5]. The detailed derivation will be presented in the next section.

III. Throughput Characterization and Optimization

In this section, we will first derive explicit expressions of the limiting state probabilities as functions of the packet transmission time τ. Based on this, we further characterize the throughput of each type of device, and then study how to optimize the network throughput by properly tuning the transmission probability of MLDs.

A. Explicit Expressions of the Limiting State Probabilities

For given τ, explicit expressions of the limiting state probabilities can be obtained in terms of the number and the transmission probability of each type of device, using (5) and (6). However, with different values of τ, the number of equations in (5) will vary, which poses significant challenges in solving the equations set and obtaining the explicit expressions of the limiting state probabilities in terms of τ.

To derive the explicit expressions of the limiting state probabilities in terms of τ, we first transform equations (5) into a set of equations solely including the limiting state probabilities of idle states. This transformation is achieved by replacing the limiting state probabilities of busy states with those of idle states. Note that with the embedded Markov chain $\boldsymbol{\mathcal{X}} = \{\boldsymbol{X}_j\}$ and (6), the limiting state probability $\tilde{\pi}_{(\mathrm{B},\mathrm{B},D)}$ with $D \neq 0$ can be written as

$$\tilde{\pi}_{(\mathrm{B},\mathrm{B},D)} = \begin{cases} \tau_{(\mathrm{B},\mathrm{B},D)}(1-\rho_{S2})\tilde{\pi}_{(\mathrm{B},\mathrm{I},D-1)}, & D > 0, \\ \tau_{(\mathrm{B},\mathrm{B},D)}(1-\rho_M\rho_{S1})\tilde{\pi}_{(\mathrm{I},\mathrm{B},D+1)}, & D < 0. \end{cases} \tag{9}$$

For the remaining steady-state probability of busy states $(\mathrm{B}, \mathrm{B}, 0)$, the following equation holds:

$$\sum_{\boldsymbol{\mu} \in \mathbb{S}} \Pr\{\text{the network state is } \boldsymbol{\mu} \text{ at time slot } t\} = 1. \tag{10}$$

[5]We refer to the States where at least one of the links is idle, such as $(\mathrm{I}, \mathrm{I}, 0)$, as *idle states*, while the remaining States are referred as *busy states*.

From (10), we have

$$\tilde{\pi}_{(\mathrm{B},\mathrm{B},0)} = 1 - \sum_{\boldsymbol{\mu} \in \mathbb{S},\ \boldsymbol{\mu} \neq (\mathrm{B},\mathrm{B},0)} \tilde{\pi}_{\boldsymbol{\mu}}. \tag{11}$$

With (9) and (11), (5) can be organized into the following matrix form:

$$\mathbf{y} = \mathbf{A}\mathbf{y} + \mathbf{b}, \tag{12}$$

where $\mathbf{y}$ is the vector of the limiting state probabilities of idle states and $\mathbf{b}$ is a constant vector. $\mathbf{y}$ and $\mathbf{b}$ are

$$\mathbf{y} = \left[\tilde{\pi}_{(\mathrm{I},\mathrm{I},0)}, \tilde{\pi}_{(\mathrm{I},\mathrm{B},0)}, \cdots, \tilde{\pi}_{(\mathrm{I},\mathrm{B},1-\tau)}, \tilde{\pi}_{(\mathrm{B},\mathrm{I},0)}, \cdots, \tilde{\pi}_{(\mathrm{B},\mathrm{I},\tau-1)}\right]^{\mathrm{T}} \tag{13}$$

and $\mathbf{b} = \left[\frac{1}{\tau}, 0, \cdots, 0, 0, 0\right]^{\mathrm{T}}$, respectively. $\mathbf{A}$ is the coefficient matrix and is shown at the top of this page, where $g(\cdot)$ and $h(\cdot)$ are

$$g(i) = -\frac{1}{\tau}(1 + (\tau - i)(1 - \rho_M\rho_{S1})) \tag{15}$$

and

$$h(i) = -\frac{1}{\tau}(1 + (\tau - i)(1 - \rho_{S2})), \tag{16}$$

respectively. With the special structure of $\mathbf{A}$, we can solve the (12) and obtain the limiting state probabilities of idle states in terms of τ. The explicit expressions of the limiting state probabilities of idle states are omitted here due to space limitations.

B. Device Throughput

Based on the limiting state probabilities of idle states characterized, the throughput of MLD can be further derived. With the derivation in Appendix A, the throughput of MLD $\hat{\lambda}^M_{out}$ can be obtained as

$$\begin{aligned}\hat{\lambda}^M_{out} =& \tau\rho_{S1}n_M q_M(1-q_M)^{n_M-1}\left(\tilde{\pi}_{(\mathrm{I},\mathrm{I},0)} + \sum_{i=0}^{1-\tau}\tilde{\pi}_{(\mathrm{I},\mathrm{B},i)}\right) + \\ & \tau\rho_{S2}n_M q_M(1-q_M)^{n_M-1}\tilde{\pi}_{(\mathrm{I},\mathrm{I},0)}.\end{aligned} \tag{17}$$

By substituting limiting state probabilities of idle states into (17), the device throughput of MLD $\hat{\lambda}^M_{out}$ can be obtained as the explicit expression of τ, transmission probabilities and the number of devices. The device throughput of SLD 1 $\hat{\lambda}^{S1}_{out}$ and SLD 2 $\hat{\lambda}^{S2}_{out}$ can also be derived in a similar way. Due to space limitations, the explicit expressions of device throughput are omitted here.

C. Maximum Network Throughput

In this subsection, we will further study how to optimize the network throughput by tuning the transmission probability of each device. Define the maximum network throughput as

$$\hat{\lambda}^{total}_{\max} = \max_{q_M, q_{S1}, q_{S2}} \hat{\lambda}^{total}_{out}. \tag{18}$$

The optimal solutions are denoted as q^*_{S1}, q^*_{S2}, and q^*_M, respectively. Based on the explicit expressions of device throughput, the optimal solutions can be obtained by numerical method.

$$\mathbf{A}=\begin{bmatrix}
\rho_M\rho_{S1}\rho_{S2}-\frac{1}{\tau} & g(1) & \cdots & g(\tau-1) & \rho_M\rho_{S1}+g(\tau) & h(1) & \cdots & h(\tau-1) & \rho_{S2}+h(\tau)\\
\rho_M\rho_{S1}(1-\rho_{S2}) & 0 & & 0 & 0 & 0 & & 0 & 1-\rho_{S2}\\
0 & \rho_M\rho_{S1} & \cdots & 0 & 0 & 0 & \cdots & 1-\rho_{S2} & 0\\
 & \vdots & \ddots & \vdots & \vdots & \vdots & \iddots & \vdots & \\
0 & 0 & \cdots & \rho_M\rho_{S1} & 0 & 1-\rho_{S2} & \cdots & 0 & 0\\
\rho_M\rho_{S2}(1-\rho_{S1}) & 0 & & 0 & 1-\rho_M\rho_{S1} & 0 & & 0 & 0\\
0 & 0 & \cdots & 1-\rho_M\rho_{S1} & 0 & \rho_{S2} & \cdots & 0 & 0\\
 & \vdots & \iddots & \vdots & \vdots & \vdots & \ddots & \vdots & \\
0 & 1-\rho_M\rho_{S1} & \cdots & 0 & 0 & 0 & \cdots & \rho_{S2} & 0
\end{bmatrix}_{((2\tau+1)\times(2\tau+1))}. \quad (14)$$

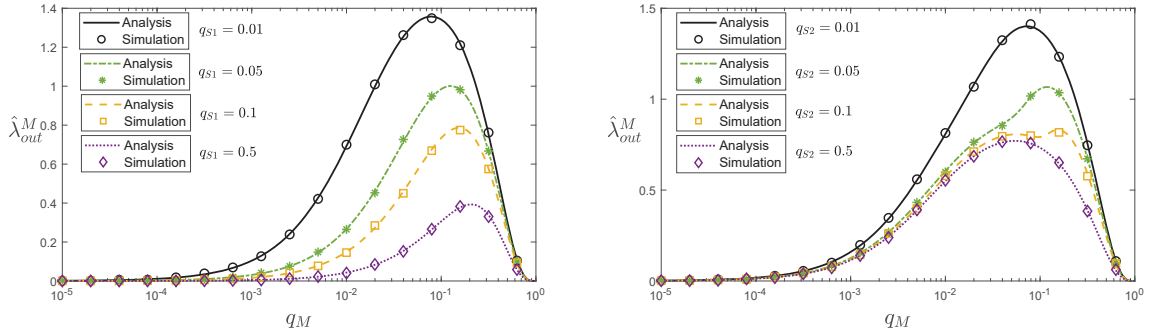

Fig. 4. (a) $\hat{\lambda}^M_{out}$ versus q_M with various q_{S1}. $n_{S1}=n_{S2}=n_M=5$, $q_{S2}=0.001$. (b) $\hat{\lambda}^M_{out}$ versus q_M with various q_{S2}. $n_{S1}=n_{S2}=n_M=5$, $q_{S1}=0.001$. τ=30.

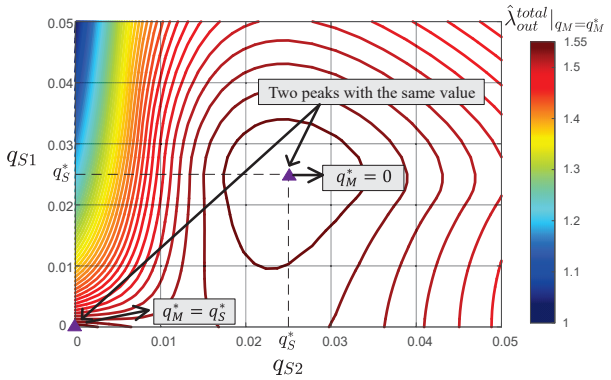

Fig. 5. Network throughput with q^*_M, $\hat{\lambda}^{total}_{out}|_{q_M=q^*_M}$, versus q_{S1} and q_{S2}, where $n_M=n_{S1}=n_{S2}=10$, $\tau=30$.

IV. Simulation Result

In this section, simulation results will be presented to verify the analysis in Section III. Note that all the simulations in this section are conducted by the event-driven simulator. In simulations, the buffer of each device is always not empty. Each device will attempt transmission in the subsequent time slot with a certain transmission probability if it senses the corresponding channel idle. Simulation results of the device throughput are obtained by calculating $\frac{\tau N}{T}$, where N is the number of packets successfully transmitted by the device over a long time period, with each simulation lasting $T=10^7$ time slots.

Let us first consider the impact of two types of SLDs—those located on the primary link and those on the secondary link—on the performance of MLDs. Fig. 4 presents how the device throughput of MLDs $\hat{\lambda}^M_{out}$ varies under various transmission probability values of legacy SLDs. Fig. 4a illustrates the effect of the SLDs on the primary channel, i.e., SLD 1, on the throughput of MLDs $\hat{\lambda}^M_{out}$. We can see from Fig. 4a that when $q_{S1}=0.01$, the maximum throughput of MLDs is greater than 1, indicating that MLDs have gained from the secondary link and achieve higher throughput than SLDs. As q_{S1} grows, i.e., more transmissions from SLD 1, the maximum throughput of MLDs decreases. This is because frequent transmissions from SLD 1 will reduce transmission opportunities for MLDs, which contend on link 1. In this case, MLDs are unable to utilize link 2 even though link 2 is idle. Fig. 4b illustrates the impact of the SLDs on the secondary channel, i.e., SLD 2, on the throughput of MLDs $\hat{\lambda}^M_{out}$. It can be seen that with the q_{S2} increasing, the maximum throughput of MLDs decreases, but the extent of the decrease is not as significant as in Fig. 4a. This is because transmissions from SLDs on the secondary channel do not affect the contention of MLDs. We can conclude that the device throughput of MLDs is more sensitive to transmissions from legacy SLDs on the primary channel, compared to transmissions from legacy SLDs on the secondary channel.

Subsequently, let us focus on the maximum throughput performance of multi-link heterogeneous networks. Fig. 5 illustrates how the network throughput with q^*_M, i.e., $\hat{\lambda}^{total}_{out}|_{q_M=q^*_M}$, varies with the transmission probabilities q_{S1}

and q_{S2}, depicted as a contour map. We can see from Fig. 5 that $\hat{\lambda}_{out}^{total}|_{q_M=q_M^*}$ has two peaks with the same value. These occur when $q_{S1} = q_{S2} = 0$ and $q_M = q_S^*$, as well as $q_{S1} = q_{S2} = q_S^*$ and $q_M = 0$, where q_S^* is the optimal transmission probability to maximize network throughput of a single-link IEEE 802.11 DCF network [13]. In other words, the maximum network throughput is achieved only when legacy SLDs or MLDs do not transmit. This indicates that the maximum throughput of heterogeneous networks is lower than that of homogeneous networks consisting solely of MLDs or legacy SLDs. We can observe that when the transmission probability of SLDs on the secondary channel is small, i.e., when q_{S2} is small, the contours along the increasing direction of q_{S1} become dense, indicating a significant decrease in the maximum network throughput. This occurs because as the primary channel experiences increased congestion, MLD fails to leverage the light-load secondary channel effectively through transmission probability adjustments, resulting in a loss of throughput benefits from the secondary channel.

V. Conclusion

In this paper, a novel model is proposed for throughput optimization of heterogeneous multi-link IEEE 802.11be networks. Based on this, explicit expressions of the throughput of MLDs and legacy SLDs are both characterized. The analysis shows that the throughput of MLDs decreases as the transmission probability of SLDs on the primary channel and the secondary channel increases. The throughput performance of MLDs is more sensitive to the transmission of legacy SLDs on the primary channel compared to the transmission of legacy SLDs on the secondary channel. We further tune the transmission probabilities of SLDs and MLDs to maximize the network throughput. Analysis results show that while MLO enhances throughput for MLDs, the maximum network throughput of heterogeneous networks is lower than that of networks comprising exclusively MLDs or SLDs.

Appendix A
Derivation of (17)

With the collision model, at most one packet can be successfully received on each channel per time slot. Therefore, the throughput of MLD, i.e., λ_{out}^M, is the sum of the probabilities of each channel has a successful packet transmission from MLDs at time t, which is

$$\hat{\lambda}_{out}^M = \sum_{k=1}^{2} \Pr\{\text{MLDs success on channel } k \text{ at } t\}. \tag{19}$$

It can be further written as[6],

$$\hat{\lambda}_{out}^M = \sum_{i=1}^{\tau}\sum_{k=1}^{2}\sum_{\boldsymbol{\mu}\in\mathbb{C}_M^{(k)}} \Pr\{\text{MLDs success on channel } k \text{ at } t-i+1| \\ \boldsymbol{\mu} \text{ at } t-i\} \cdot \Pr\{\boldsymbol{\mu} \text{ at } t-i\} \tag{20}$$

where $\Pr\{\boldsymbol{\mu} \text{ at } t\} = \tilde{\pi}_{\boldsymbol{\mu}},\ \boldsymbol{\mu} \in \mathbb{S}$. $\mathbb{C}_M^{(k)}, k \in \{1,2\}$ are the sets of channel states that allow MLDs to transmit on the channel k in the next time slot, which are given by

$$\mathbb{C}_M^{(1)} = \{(\mathrm{I},\mathrm{I},0),(\mathrm{I},\mathrm{B},0),\ldots,(\mathrm{I},\mathrm{B},1-\tau)\} \tag{21}$$

and $\mathbb{C}_M^{(2)} = \{(\mathrm{I},\mathrm{I},0)\}$, respectively. By substituting $\mathbb{C}_M^{(i)}$ into (20), (17) can be obtained.

References

[1] E. Khorov, I. Levitsky, and I. F. Akyildiz, "Current Status and Directions of IEEE 802.11be, the Future Wi-Fi 7," *IEEE Access*, vol. 8, pp. 88 664–88 688, 2020.

[2] A. A. Abdalhafid, S. K. Subramaniam, Z. A. Zukarnain, and F. H. Ayob, "Multi-Link Operation in IEEE802.11be Extremely High Throughput: A Survey," *IEEE Access*, vol. 12, pp. 46 891–46 906, 2024.

[3] C. Deng, X. Fang, X. Han, X. Wang, L. Yan, R. He, Y. Long, and Y. Guo, "IEEE 802.11 be Wi-Fi 7: New challenges and opportunities," *IEEE Commun. Surveys Tuts.*, vol. 22, no. 4, pp. 2136–2166, 2020.

[4] I. Jang, J. Choi, J. Kim, S. Kim, S. Park, and T. Song, "Channel Access for Multi-Link Operation," document IEEE 802.11-19/1144r6, Nov. 2019.

[5] Y. Seok, D. Akhmetow, D. Ho, R. Chirakar, M. Gan, I. Jang, and S. Naribole, "UL Sync Channel Access Procedure," document IEEE 802.11-20/1730r3, Nov. 2020.

[6] Á. López-Raventós and B. Bellalta, "Multi-link operation in IEEE 802.11 be WLANs," *Proc. IEEE Wireless Commun*, vol. 29, no. 4, pp. 94–100, 2022.

[7] J. Zhang, Y. Gao, X. Sun, W. Zhan, P. Liu, and Z. Guo, "Synchronous Multi-Link Access in IEEE 802.11 be: Modeling and Network Sum Rate Optimization," in *Proc. IEEE ICC*, 2022, pp. 2309–2314.

[8] N. Korolev, I. Levitsky, and E. Khorov, "Analyses of NSTR Multi-Link Operation in the Presence of Legacy Devices in an IEEE 802.11 be Network," in *Proc. IEEE Conf. Standards Commun. Netw (CSCN)*, 2021, pp. 94–98.

[9] ——, "Analytical Model of Multi-Link Operation in Saturated Heterogeneous Wi-Fi 7 Networks," *IEEE Commun. Lett.*, vol. 11, no. 12, pp. 2546–2549, 2022.

[10] T. Song and T. Kim, "Performance Analysis of Synchronous Multi-Radio Multi-Link MAC Protocols in IEEE 802.11be Extremely High Throughput WLANs," *Applied Sciences*, vol. 11, no. 1, 2021.

[11] S. Jung, S. Choi, H. Kim, Y. Yoon, and H.-K. Son, "Modeling the Coexistence Performance between Wi-Fi 7 and legacy Wi-Fi," in *IEEE Netw. Oper. Manage. Symp.*, 2024, pp. 1–4.

[12] G. Bianchi, "Performance Analysis of the IEEE 802.11 Distributed Coordination Function," *IEEE J. Selected Areas Comm.*, vol. 18, no. 3, pp. 535–547, 2000.

[13] L. Dai and X. Sun, "A Unified Analysis of IEEE 802.11 DCF Networks: Stability, Throughput, and Delay," *IEEE Trans. Mobile Computing.*, vol. 12, no. 8, pp. 1558–1572, 2012.

[6]We adopt the short notation: $\Pr\{\boldsymbol{\mu} \text{ at } t\} = \Pr\{\text{channel state is } \boldsymbol{\mu} \text{ at } t\}$, where $\boldsymbol{\mu} \in \mathbb{S}$.